Brassinosteroids modulate the efficiency of plant immune responses to microbe-associated molecular patterns

Youssef Belkhadir[a,b,1], Yvon Jaillais[a,b,1], Petra Epple[c], Emilia Balsemão-Pires[a,b,2], Jeffery L. Dangl[c,d,3], and Joanne Chory[a,b,3]

[a]Plant Biology Laboratory and [b]Howard Hughes Medical Institute, Salk Institute for Biological Studies, La Jolla, CA 92037; and [c]Howard Hughes Medical Institute, Department of Biology, and [d]Department of Microbiology and Immunology, Curriculum in Genetics, Carolina Center for Genome Sciences, University of North Carolina, Chapel Hill, NC 27599

Contributed by Joanne Chory, August 6, 2011 (sent for review June 16, 2011)

Metazoans and plants use pattern recognition receptors (PRRs) to sense conserved microbial-associated molecular patterns (MAMPs) in the extracellular environment. In plants, the bacterial MAMPs flagellin and elongation factor Tu (EF-Tu) activate distinct, phylogenetically related cell surface pattern recognition receptors of the leucine-rich repeat receptor kinase (LRR-RK) family called FLS2 and EF-Tu receptor, respectively. BAK1 is an LRR-RK coreceptor for both FLS2 and EF-Tu receptor. BAK1 is also a coreceptor for the plant brassinosteroid (BR) receptor, the LRR-RK BRI1. Binding of BR to BRI1 primarily promotes cell elongation. Here, we tune the BR pathway response to establish how plant cells can generate functionally different cellular outputs in response to MAMPs and pathogens. We demonstrate that BR can act antagonistically or synergistically with responses to MAMPs. We further show that the synergistic activities of BRs on MAMP responses require BAK1. Our results highlight the importance of plant steroid homeostasis as a critical step in the establishment of plant immunity. We propose that tradeoffs associated with plasticity in the face of infection are layered atop plant steroid developmental programs.

brassinosteroid signaling | plant immune system signaling | signaling crosstalk

Innate immune systems of plants and animals rely on pattern recognition receptors (PRRs) to produce an appropriate physiological response upon detection of nonself molecules (1, 2). PRRs respond to conserved microbe-associated molecular patterns (MAMPs) (1, 2). In *Arabidopsis*, the majority of PRRs are leucine-rich repeat (LRR)-receptor kinases (RKs). MAMPs often play no role in pathogenesis, but rather are indispensable for core microbial functions (1). MAMPs are typically conserved among diverse sets of pathogens. Well studied MAMPs in plant immune system studies include a 22-aa peptide derived from flagellin (flg22) and a bioactive 18-aa peptide derived from the translational elongation factor Tu (elf18), peptidoglycans (PGNs), and chitin, a component of fungal cell walls. MAMPs elicit a suite of defense responses including the accumulation of reactive oxygen intermediates, deposition of callose, large-scale transcriptional reprogramming, and biosynthesis of microstatic and/or microcidal secondary metabolites. This response constitutes MAMP-triggered immunity (MTI), which is sufficient to slow or halt microbial proliferation (1–3).

Recent studies have unveiled a web of interactions between the plant immune system and growth regulating hormones like auxin, gibberellins, and ethylene (2). However, there is little evidence for direct physical convergence points linking hormone and defense response signaling systems (4). One convergence point that could link growth-promoting hormone responses to MAMP signaling is the LRR-RK BRI1-Associated Kinase 1 (BAK1) (2, 5). BAK1 was identified as an interactor of the LRR-RK Brassinosteroid (BR)-Insensitive 1 (BRI1), which binds brassinolide (BL), the most potent steroid hormone in plants. Upon BL binding, BRI1 autophosphorylates and activates BAK1 by transphosphorylation, thereby enhancing signaling competency through reciprocal BRI1 transphosphorylation (6). Similarly, Flagellin-Sensitive 2 (FLS2), the receptor for the bacterial flagellum peptide flg22, associates with BAK1 immediately upon ligand binding (7). BAK1 recruitment to specific cell surface signaling systems involve its extracellular LRRs and differential phosphorylation-dependent events for proper signal transduction (7–9). Hence, BAK1 is an adapter recruited downstream of ligand perception for several cell surface signaling pathways. To date, BAK1 function in innate immunity appears to be genetically independent from its function in BR signaling (10). Here, we revisit the interplay between the plant immune system and plant steroids and demonstrate that BR biosynthesis and signaling can be rate-limiting modulators of BAK1-mediated MAMP responses.

Results

Maintenance of BR Homeostasis Is Critical for flg22-Induced MTI Signaling. Exogenous application of extremely high concentrations of BL unmasked a role for BRs in the control of a range of weak immune responses (11). This function of BR as a modulator of plant immunity is uncharacterized to our knowledge. We used transgenic *Arabidopsis* plants ectopically overexpressing *DWARF4* (*35S::DWF4*) to investigate whether PRR signaling is altered under conditions of excess BR biosynthesis (12). *DWF4* encodes a C-22 hydroxylase, which is a rate-limiting step of BL biosynthesis. *35S::DWF4* plants display elongated organ phenotypes, and dramatically reduced responses to flg22 (Fig. 1 *A* and *B* and Fig. S1). Thus, increasing the endogenous pool of bioactive BR antagonizes flg22-induced responses. Loss-of-function BR biosynthetic or signaling mutants display dramatic changes in cell elongation, resulting in severe dwarfism (13), complicating assays for immune system function. We therefore transiently reduced BR biosynthesis by using brassinazole (BRZ), a triazole compound that reversibly and specifically blocks DWF4 activity (14). To monitor flg22 output in the root, we used a *CYP71A12* gene–GUS reporter transgenic line (*pCYP71A12::GUS*) (15) (Fig. 1*C*). We subjected *pCYP71A12::GUS* seedlings to BRZ treatment and monitored *GUS* reporter gene activation upon flg22 treatment. In the presence of BRZ, *pCYP71A12* response to flg22 was greatly diminished (Fig. 1*C*). Removal of BRZ before flg22 treatment

Author contributions: Y.B., Y.J., P.E., E.B.-P., J.L.D., and J.C. designed research; Y.B., Y.J., P.E., and E.B.-P. performed research; Y.B., Y.J., P.E., E.B.-P., J.L.D., and J.C. analyzed data; and Y.B., Y.J., P.E., J.L.D., and J.C. wrote the paper.

The authors declare no conflict of interest.

[1]Y.B. and Y.J. contributed equally to this work.

[2]Present address: Department of Genetics, Laboratório de Genômica Funcional e Transdução de Sinal, Universidade Federal do Rio de Janeiro, 21944-970, Rio de Janeiro, Brazil.

[3]To whom correspondence may be addressed. E-mail: chory@salk.edu or dangl@e-mail.unc.edu.

This article contains supporting information online at www.pnas.org/lookup/suppl/doi:10.1073/pnas.1112840108/-/DCSupplemental.

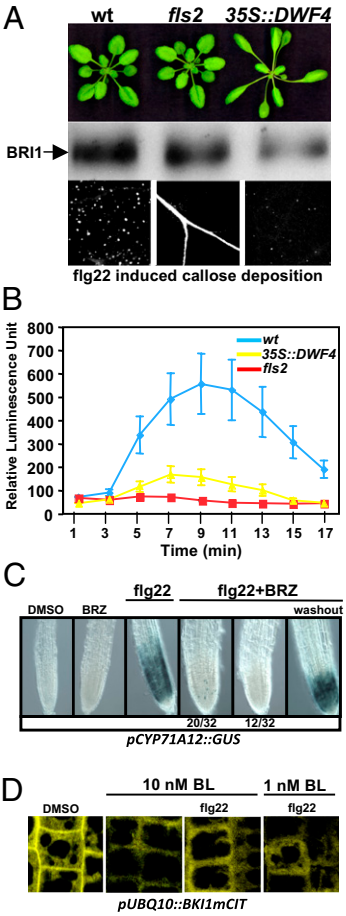

Fig. 1. BR biosynthesis modulates MAMP signaling. (*A*) *Top*: Images representative of *Arabidopsis* WT Col-0, *fls2*, and *35S::DWF4*. *Middle*: Microsomal protein extracts prepared from genotypes listed at the top were subjected to anti-BRI1 immunoblot analysis. *Bottom*: Aniline blue-stained callose deposits in the leaves of the genotypes listed at the top treated with 1 μM flg22. (*B*) Oxidative burst triggered by 1 μM flg22 in WT Col-0 (blue), *fls2* (red), and *35S::DWF4* (yellow) leaf discs measured in relative luminescence units. (*C*) GUS stains of *CYP71A12::GUS* line. Seedlings grown in the presence or absence of 5 μM BRZ were left untreated or treated with 1 μM flg22 for 12 h before GUS staining. Washout indicates removal of BRZ during flg22 treatment. Numbers at the bottom indicate the number of roots tested that fall into each category among the 32 roots assayed when BRZ was used in conjunction with flg22. In this assay, 20 roots of 32 displayed a highly attenuated response in the form of small blue spots. (*D*) Subcellular dynamics of BKI1 upon BL treatment is not affected by flg22 treatments. Subcellular localization of BKI1mCIT is shown in root meristem epidermal cells. BKI1mCIT is localized to the PM and cytosol in the absence of BL treatment (i.e., DMSO) and relocates rapidly from the PM to the cytosol following BL application. Note that BKI1 relocalization to the cytosol after BL treatment is not affected by flg22 treatment even when low concentrations of BL are used (10 nM and 1 nM). This experiment was repeated two times with similar results.

(i.e., washout) restored full induction of *pCYP71A12-GUS* (Fig. 1*C*). Thus, transient depletion of endogenous BR pools strongly suppresses flg22 signaling in root cells. We tested whether flg22 signaling can also modulate BR responses. We used displacement of the BRI1 inhibitory protein BKI1 from the plasma membrane (PM) as a readout of early BR activation (16). Our results show that sustained activation of the FLS2 pathway could not block BKI1 displacement from the PM, even at low doses of BL (Fig. 1*D*). Thus, sustained FLS2 signaling does not modulate early BR signaling outputs. Collectively, our results suggest the existence of one-way cross-talk between the balanced activities of BR biosynthesis and FLS2 signaling.

Overexpression of BRI1 Antagonizes BAK1-Mediated PRR Signaling and Cell Death. Next, we tested whether BR signaling could be limiting for MTI responses when signaling is activated via BRI1. Plants expressing BRI1 under the control of the strong CaMV 35S promoter (*35S::BRI1*) failed to respond to flg22 treatment, similar to *bak1* and *fls2* plants (Fig. 2 *A* and *B* and Figs. S2 and S3). We extended these findings to signaling pathways activated by two additional MAMPs (elf18 and PGN), which also require BAK1 for signaling (Fig. 2*B*). Conversely, *35S::BRI1* plants displayed WT responses to chitin, a MAMP that triggers BAK1-independent responses. Hence, only BAK1-mediated MTI is impaired in *35S::BRI1* plants. The lack of BAK1-mediated MTI response in *35S::BRI1* plants could be the consequence of a limiting pool of BAK1 that is unavailable for MAMP signaling. To test this, we moderately increased *BAK1* dosage by introducing a *BAK1-HA* transgene into *35S::BRI1* plants and tested flg22 responsiveness (Fig. 3*A*). The presence of extra copies of *BAK1* restored flg22 sensitivity in *35S::BRI1* plants. Thus, there is a direct link between restoration of FLS2 function and BAK1 dosage in the specific context of heightened BRI1 levels. Collectively, our results demonstrate that increased BR signaling triggered by BRI1 overexpression can antagonize the activities of at least three BAK1-dependent MAMP signaling pathways.

In some instances, our *BAK1-HA* transgenic plants displayed morphological phenotypes reminiscent of those associated with plants that develop spontaneously plant cell death (17). To confirm our observations, we used the native promoter to express a mCitrine epitope-tagged *BAK1* in WT (*BAK1mCIT*) and *bak1* (*BAK1mCIT bak1*) plants. *BAK1mCIT* accumulates to equivalent levels in *bak1* and WT plants and complements the BR- and flg22-dependent phenotypes of *bak1* plants (9) (Fig. S4). The increased dose of *BAK1* in WT, but not in *bak1*, resulted again in

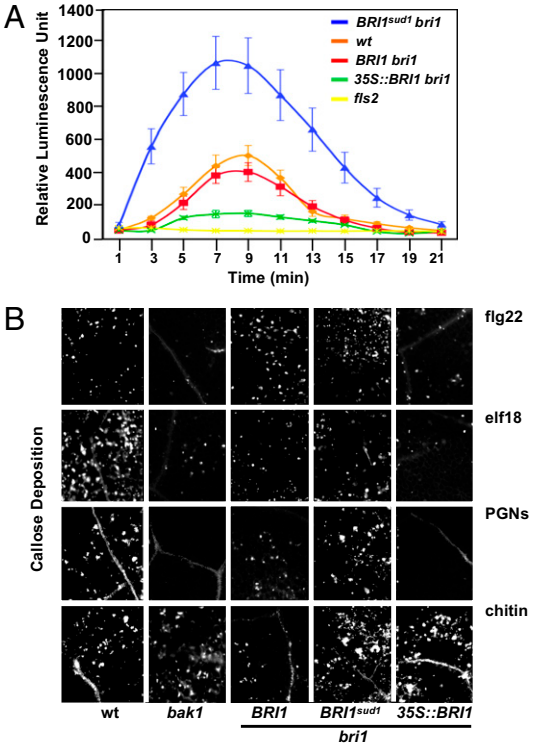

Fig. 2. BR signaling modulates MTI. (*A*) Oxidative burst in relative luminescence units, triggered by 1 μM flg22 in leaf discs of the genotypes listed on the top right corner. (*B*) Aniline blue-stained callose deposits in leaves of the genotypes listed at the bottom treated with 1 μM flg22 or elf18 and 100 μg/mL of PGNs or chitin.

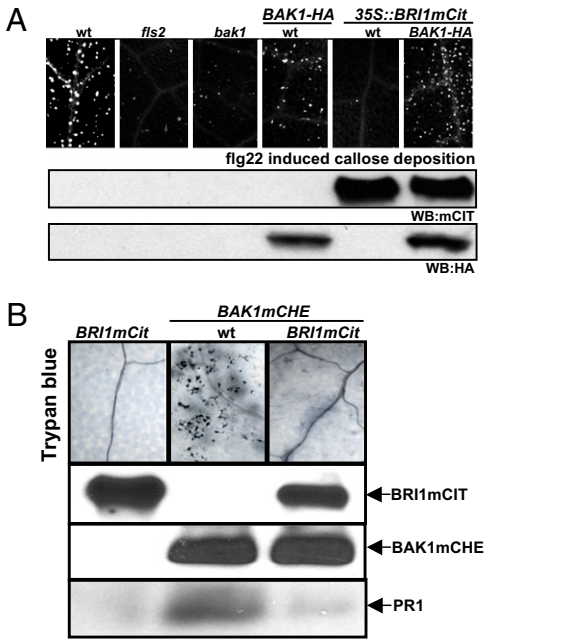

Fig. 3. Overexpression of BRI1 antagonizes BAK1-mediated MAMP and cell death responses. (*A*) *Top*: Aniline blue-stained callose deposits in leaves of the genotypes listed treated with 1 μM flg22. *Middle*, *Bottom*: Microsomal protein extracts prepared from the genotypes listed at the top were subjected to an anti-GFP (WB:mCIT) or to an anti-HA (WB:HA) immunoblot analysis to detect the accumulation of mCit or HA tagged proteins. (*B*) *Top*: Trypan blue stain of leaves from the genotypes listed at the top. Genotypes of parental and resulting F1 lines are indicated at the top. The control lane (*Left*) represents F1 plants obtained through a cross between *BRI1mCIT* and Col-0. Trypan blue stains of F1 plants from the following crosses: *BRI1mCit* × Col-0 (control; *Left*), *BAK1mCHE* × Col-0 (*Middle*), and *BAK1mCHE* × *BRI1mCit* (*Right*). Two middle panels: Microsomal protein extracts were prepared from the genotypes listed at the top and subjected to anti-GFP and anti-DsRED immunoblot analysis to detect mCitrine and mCherry tagged proteins, respectively. *Bottom*: Total protein extracts were prepared from the genotypes listed at the top and were subjected to anti-PR1 immunoblot analysis.

plants displaying morphological phenotypes reminiscent of spontaneously discrete necrotic lesions (17), which we confirmed with trypan blue staining in *BAK1mCIT* plants (Fig. S4). Plants displaying ectopic cell death often accumulate constitutively Pathogenesis-Related (*PR*) proteins and are called *cpr* mutants (17). PR1 protein accumulated to readily detectable levels in *BAK1mCIT* plants but not in *BAK1mCIT bak1* plants (Fig. S4). Thus, increased BAK1 dosage drives inappropriate cell death responses. By contrast, we never observed plants displaying a *cpr* morphology when the levels of a dominant allele of *BAK1*, *bak1*^{elg}, were increased (Fig. S4). Because the *elg* mutation generates a BAK1 variant that more strongly associates with BRI1 (9), we reasoned that the phenotypes associated with heightened BAK1 levels could be suppressed by altering *BRI1* gene dosage. We used transgenic plants expressing mCherry epitope-tagged BAK1 under its native promoter in Columbia-0 (Col-0) WT (*BAK1mCHE*) (16). *BAK1mCHE* plants displayed phenotypes similar to those observed in *BAK1mCIT* plants. Thus, the inappropriate cell death phenotypes observed in our transgenic lines are specific to BAK1 levels, rather than being related merely to the BAK1 epitope tag. We crossed *BAK1mCHE* plants to WT *BRI1mCIT* plants and monitored ectopic cell death and PR protein accumulation. Importantly, increasing the dose of *BRI1* in the context of heightened BAK1 levels suppressed almost entirely the BAK1 overexpression phenotypes (Fig. 3*B*). Thus, increased BR signaling mediated by BRI1 overexpression can antagonize the inappropriate cell death signaling triggered by increased BAK1 dosage.

***BRI1*^{sud1} Plants Display Enhanced flg22-Induced Signaling.** Our data suggest that the BR-independent functions of BAK1 in plant immunity can collide with its BR-dependent role in growth and development when BRI1 dosage is increased. To test whether the loss of MAMP signaling in *35S::BRI1* plants was a result of increased BRI1 levels, or of increased BRI1 activity, we used the hypermorphic *BRI1*^{sud1} allele (Fig. S2). *BRI1*^{sud1} plants phenocopied every BR-dependent morphological aspect of *35S::BRI1* plants, but displayed dramatically increased responses to flg22 (Fig. 2*A* and Figs. S2 and S3*A*). BRI1^{sud1} protein accumulates to approximately WT levels (Fig. S2). Thus, the antagonistic effects on MAMP signaling we observed in *35S::BRI1* plants are likely the consequence of increased levels of BRI1, and not of increased intrinsic BRI1 signaling activity.

The unexpected result that *BRI1*^{sud1} plants displayed enhanced responses to flg22 treatment prompted us to investigate this response during a plant–microbe interaction. We used the hemibiotrophic bacterial pathogen, *Pseudomonas syringae* pv. *tomato* (*Pto*) DC3000, and the isogenic *Pto* DC3000*hrcC* mutant, which is deficient in its type III secretion system (T3SS). The T3SS allows bacterial effectors delivery to host cells for maximal virulence (18). Flg22 infiltrated into *Arabidopsis* leaves induces MTI that can inhibit *P. syringae* growth (19). Flg22 treatments weakly inhibited *Pto* DC3000 growth on all genotypes tested, with the exception of *BRI1*^{sud1}, which exhibited enhanced response, and *fls2*, which, as expected, exhibited none (Fig. S3). When *Pto* DC3000*hrcC* was infiltrated together with flg22, bacterial growth was inhibited approximately 10 fold on BRI1 plants and approximately 100 fold on *BRI1*^{sud1} plants (Fig. 4). Thus, the FLS2 signaling pathway in *BRI1*^{sud1} plants can be further stimulated and acts effectively to limit bacterial growth. In contrast, we did not observe flg22-dependent inhibition of *Pto* DC3000*hrcC* growth on *35S::BRI1* or *bak1* plants. We propose that the loss of FLS2 signaling in *35S::BRI1* plants is likely the consequence of the inability of BAK1 to contribute to flg22 signaling. Our results with DC3000*hrcC* imply that increased BR signaling via *BRI1*^{sud1} primes BR and flg22 signaling through BAK1. Accordingly, when BRI1 levels are increased (i.e., *35S::BRI1*) the stimulatory effects of BR on flg22 signaling are negated, presumably by increased recruitment of BAK1 to BRI1.

We used three molecular readouts to monitor the basal activity of FLS2 in *BRI1*^{sud1} plants: (*i*) its phosphorylation status, (*ii*) its internalization and subsequent disappearance, and (*iii*) the induction of downstream target genes (20, 21). By using an

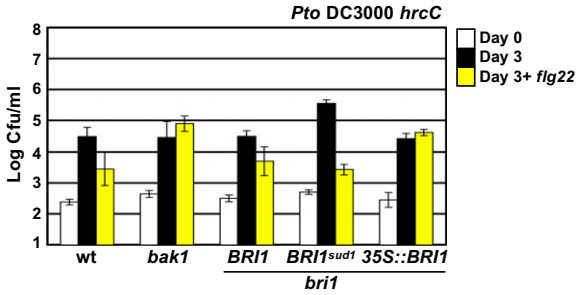

Fig. 4. BR signaling modulates flg22-dependent disease resistance. Growth of *Pto*DC3000 *hrcC* was measured in the genetic backgrounds indicated at the bottom of the chart. Four-week-old plants were infiltrated with 10^5 cfu/mL *Pto*DC3000 *hrcC* in the absence (black bars) or presence (yellow bars) of 1 μM flg22. The number of bacteria per area of leaf was determined at 0 and 3 d postinoculation (*Experimental Procedures*) and plotted on a log10 scale. Values are mean cfu/mL ± 2 SE.

anti-FLS2 antibody, we immunoprecipitated FLS2 from unchallenged WT and *BRI1*^{sud1} plants (Fig. S5). We noted that FLS2 in *BRI1*^{sud1} plants is already phosphorylated in the absence of flg22, and accumulates to lower levels (Fig. S5). Thus, the basal activity of FLS2 is increased in *BRI1*^{sud1} plants in the absence of flg22, and FLS2 accumulation is not rate-limiting for the enhanced flg22 responses. We could not observe reliably increased internalization of FLS2 in endosomal compartments in *BRI1*^{sud1} plants (Fig. S5) (21). This suggests that the stimulatory effect of BRI1^{sud1} on FLS2 is mild.

MAMP signals perceived at the cell surface often terminate on the promoters of *WRKY* transcription factor genes (20). To further confirm that FLS2 signaling is primed in *BRI1*^{sud1} plants, we quantified the expression levels of several *WRKY* genes. All the *WRKY* genes tested showed a relative increase in their expression levels in *BRI1*^{sud1} plants (Fig. S5). This change in *WRKY* gene expression might not specifically reflect FLS2 signaling, as MAMP-driven transcriptional reprogramming is generic and results in the activation of a largely overlapping set of defense genes (1). Rather, we envision that the induction of basal defense genes in unchallenged *BRI1*^{sud1} plants is a general consequence of inappropriate BAK1-mediated signaling. To test this hypothesis, we created isogenic lines expressing *BRI1*^{sud1} in the WT and *bak1* genetic backgrounds and looked at the steady-state expression of *WRKY* genes in 30 independent T1 plants. Our results demonstrated that the effects of *BRI1*^{sud1} on defense gene expression are *BAK1*-dependent, whereas the effects on cell elongation are not (Fig. 5*A*). We attribute this to the fact that BAK1 function in BR signaling can be partially compensated by the LRR-RK Somatic Embryogenesis Receptor Kinase 1 (SERK1) (22). To further confirm that the enhanced flg22 responses observed in *BRI1*^{sud1} plants are *bak1*-dependent, we assayed flg22-mediated seedling growth inhibition (SGI) in *BRI1*^{sud1} *bak1* double-mutant plants (Fig. 5*B*). *BRI1*^{sud1} *bak1* plants showed no SGI, similar to *bak1* plants. Thus, the increased flg22-dependent SGI response in *BRI1*^{sud1} is *BAK1*-dependent. Together, our results indicate that the increased activity of the BR signaling pathway, triggered by the *BRI1*^{sud1} variant, requires BAK1 to enhance MAMP-dependent responses.

BR Signaling Mediates BAK1-Dependent Changes in Susceptibility to Obligate Biotrophic Pathogen. To test if imbalance in BR signaling could be exploited by obligate biotrophic pathogens to further their fitness and growth, we challenged *BRI1*^{sud1} plants with the virulent oomycete *Hyaloperonospora arabidopsidis* (*Hpa*) isolate Noco2. *bak1* displayed a significant increase in resistance to the virulent *Hpa* isolate Noco2 in comparison with WT Col-0 (Fig. 5 *C* and *D* and Table S1) (23). Sporulation on *BRI1*^{sud1} was not different from that of *BRI1* plants (Fig. 5 *C* and *D* and Table S1). Morphologically, *BRI1* plants display very mild BR gain-of-function phenotypes, possibly because of accumulation greater than WT endogenous levels. *BRI1* and *BRI1*^{sud1} allowed reproducible, strong increases in sporulation compared with Col-0 (Fig. 5 *C* and *D* and Table S1).

Thus, an increase in BR signaling driven by the extra gene dosage of *BRI1* or the hypermorphic activity of *BRI1*^{sud1} enhances susceptibility to Noco2. Importantly, this effect was more pronounced on the first true leaves, organs in which BR-driven cell elongation programs are hyperactive (Fig. 5*D*). Furthermore, the increased sporulation of Noco2 driven by heightened BR signaling was *BAK1*-dependent, as the *BRI1 bak1* and *BRI1*^{sud1} *bak1* double mutants supported dramatically less sporulation. These plants supported even less sporulation than *bak1* (Fig. 5 *C* and *D* and Table S1). Thus, increased BR signaling in the absence of *bak1* is able to suppress Noco2 sporulation. Importantly, BRI1 and BRI1^{sud1} accumulated to approximately equivalent levels in Col-0 and *bak1* plants (Fig. S6). *RPP4*-mediated resistance to the avirulent *Hpa* isolate Emwa1 was compromised in a *BAK1*-dependent manner in *BRI1* and *BRI1*^{sud1} plants as well (Fig. S6 and Table S1) (24). These findings suggest that a slight increase in BR signaling in the presence of BAK1 enhances susceptibility to *Hpa*, whereas the same slight increase in BR signaling reduces sus-

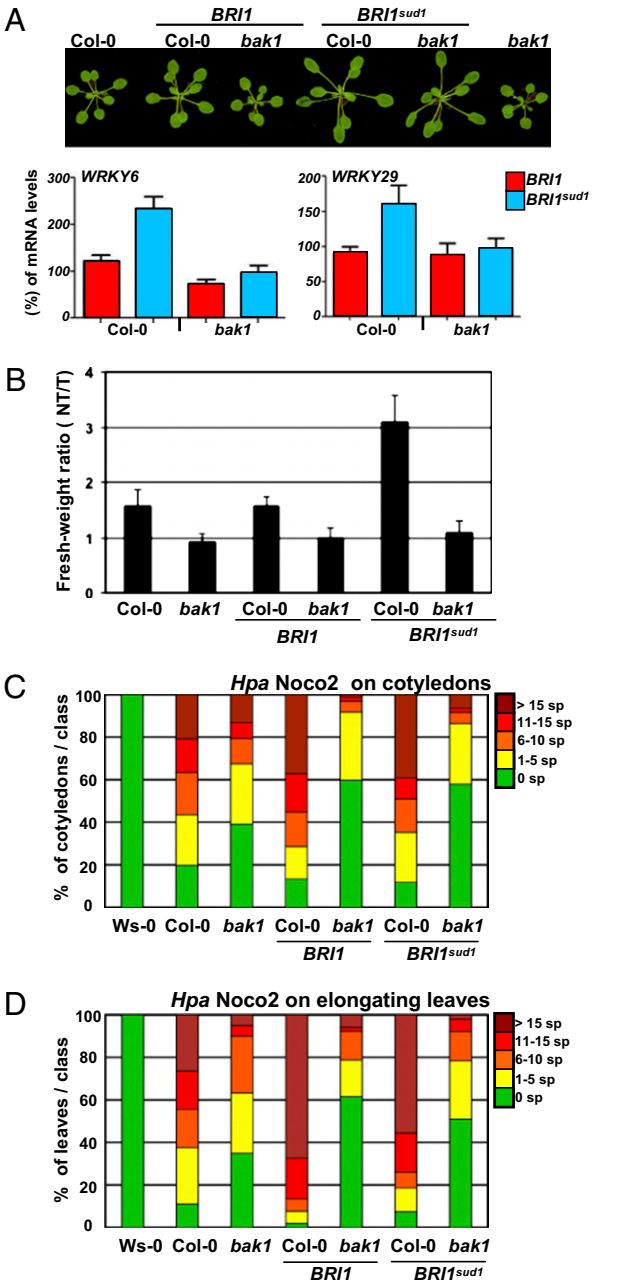

Fig. 5. Enhanced BR signaling promotes growth of an obligate biotrophic pathogen in a BAK1-dependent manner. (*A*) Images of representative rosette stage *Arabidopsis* plants with genotypes listed at the top. *Bottom*: Quantitative RT-PCR analyses of *WRYK6 and WRKY29* transcripts from plants expressing *BRI1* (red) or *BRI1*^{sud1} (blue) in WT or *bak1* genetic backgrounds. (*B*) Average fresh-weight ratio of seedlings grown in water (NT) or 1 μM flg22 (T). Genotypes are listed at the bottom. (*C* and *D*) Twelve-day-old seedlings of the genetic backgrounds indicated at the bottom of the chart were inoculated with conidiospores of the virulent *Hpa* isolate Noco2 at 32,000 spores/mL. Sporangiophores were counted 4 d after inoculation on cotyledons (*C*) and on first true leaves (*D*) for each of the indicated genetic backgrounds. Means, sample sizes, and 2 × SE are presented in Table S1. The experiment was repeated twice. sp, sporangiophores per cotyledon (*C*) or sporangiophores per leaf (*D*).

ceptibility in *bak1*. This is consistent with our proposal that BAK1 can act as mediator for the activities of BRs on PRR responses but further indicates that BR can also act on plant defenses by using a BAK1-independent mechanism.

Discussion

Despite the involvement of various hormone-regulated responses in plant defense, relatively little is known about the molecular mechanisms that connect pathogen perception to ongoing developmental programs in the infected cell or organ (2, 4). We studied the interaction of growth promotion by BRs with plant immune system activities by taking advantage of the fact that BRI1 activity and BR concentrations are highly regulated, rate-limiting factors for BR-dependent responses. We therefore could manipulate BR signaling to dissect its overlap with the plant immune system. Our data suggest a model in which BRs can reset or prime MTI responses. Our model refines current models of independent signaling functions for BR and MTI outputs, and suggests that there is a potential physiological intersection between the signaling pathways that control body size and innate immunity in plants (10). As such, pathway cross-communication simply cannot be tackled by studying signaling systems in isolation (25, 26).

In WT *Arabidopsis*, BRs and BRI1 exist at concentrations that allow cells to easily modulate their elongation state in response to challenging environmental conditions via BR synthesis (26). However, to set endogenous BR levels and BRI1 sensitivity to a particular activity range, BR biosynthesis is tightly modulated by a feedback regulatory loop controlled by BR signaling (27). A deviation from this range could have detrimental consequences on the adaptive plasticity of plants. In light of our model, we speculate that this homeostatic loop also coordinates BR biosynthesis and signaling to keep the plant immune system properly sensitized. Atop this BR feedback regulatory loop, BR homeostasis is also achieved through circadian control and other environmental factors (e.g., light, temperature, and the circadian clock) (28). Our results showing that flg22-mediated responses can be modified by the availability of BRs suggest that the temporal integration of the BR pathway could directly influence the efficiency of MTI in a circadian manner. Thus, our results build on recent findings revealing a fundamental link between the circadian clock and plant immunity (29). We posit the existence of a narrow range of BR concentrations that sets the immune response for rapid deployment. It will be important to determine precisely how the inducible responses of the plant immune system interact with BR biosynthesis and signaling to integrate defenses responses over normal growth and development programs.

Because MTI and BR responses are coupled, we predict that BR and MAMP signaling pathways do not respond to ligand concentrations directly but rather indirectly, via the ratios of respective ligand concentrations. BAK1 has the attributes required to couple the relative phenotypic outputs in this model: BAK1 interacts physically with several PRRs and BRI1 (5, 20). BAK1 does not appear to bind ligand, and thus cannot directly measure ligand concentrations (13). BAK1 pools are dynamic and, most importantly, our data show that BAK1 dosage is important for two different signaling events to occur in a sustained way. Our data showing that BRI1 overexpression antagonizes BAK1-mediated MAMP signaling and inappropriate BAK1-mediated cell death is in agreement with our proposed model. We suggest that the capacity of BAK1 to evaluate the ratios of ligands can be skewed by ligand-independent activation of BR signaling: overexpressed BRI1 (*35S::BRI1*) could possibly titrate BAK1 from PRRs, activating BR response by mass action. Accordingly, when intracellular BR levels are increased (e.g., in *35S::DWF4*), the inhibitory effects of BRs on FLS2 could take place through increased recruitment of BAK1 to BRI1. However, Albrecht and colleagues (30) have demonstrated that exogenous application of high concentrations of BR inhibits flg22-dependent signaling via a BAK1-independent mechanism. Thus, the reduced flg22 responses associated with an increase in endogenous BR levels through *DWF4* overexpression could also operate through a BAK1-independent mechanism. However, comparing and understanding the effects of endogenously increased BR pools and exogenously applied BRs on flg22 response may be complex. For instance, exogenously applied BRs taken up by *Arabidopsis* roots can rescue shoot dwarfism, yet, it is known that BRs synthesized in the roots of WT plants cannot rescue the shoot dwarfing phenotype of a BR biosynthetic mutant (31). Nonetheless, our data complement those of Albrecht et al., who also clearly demonstrate that BR and MTI signaling are coupled in a unidirectional antagonistic manner (30).

Collectively, our results demonstrate that BR signaling can dictate the output of a plant–pathogen interaction. Hence, pathogens may perturb PRRs to exploit their crosstalk with BR signaling. To test this, we challenged our BR response gain-of-function plants with oomycetes and bacterial and fungal plant pathogens. The poised activation state of $BRI1^{sud1}$ led to enhanced susceptibility to hemibiotrophic pathogens, despite enhanced MTI output responses. This enhanced susceptibility to hemibiotrophic pathogens was not apparent in plants in which BR signaling was achieved through increased BRI1 dosage. In contrast, very slight activation of the BR pathway triggered both BAK1-dependent and BAK1-independent changes during interactions with an obligate biotrophic pathogen. This is consistent with our proposal that BAK1 can act as mediator for the synergistic activities of BRs. These data are also consistent with the work of Albrecht et al. (30), who propose that BR signaling modulates plant immunity in a BAK1-independent manner. We propose that biotrophic pathogens have evolved virulence mechanisms to detect or create physiological states in which BR concentrations are optimal for pathogen success, perhaps centered on the modification of BR biosynthesis or signaling (32). Further studies aimed at understanding how BRs impact the concerted array of plant hormone signaling relationships with innate immune function will be instrumental to determine how the plant cell integrates normal growth signals with immune system function.

Experimental Procedures

Confocal Microscopy. flg22 and BL treatments were as described previously (9). Confocal microscopy was performed with a Leica SP/2 inverted microscope, and image analysis was performed as previously described (16).

Protein Analysis. Equal loading was ensured by Bradford protein quantification before loading. Monoclonal anti-GFP (Roche), anti-HA (Roche), and polyclonal anti-CHERRY (DsRed polyclonal; Clontech) were used at a dilution of 1:2,000. Polyclonal anti-PR1 antibodies were provided by Dan Kliebenstein (University of California, Davis, CA) and used at a dilution of 1:5,000.

MAMP Responses Assays. These assays were as described (9). *pCYP71A12::GUS* staining assays following treatment with 1 μM flg22 were as described previously (15). Seedlings grown in the presence or absence of 5 μM BRZ (Chemiclones) were untreated or treated with 1 μM flg22 for 12 h before GUS staining. Washout indicates removal of BRZ during a short period before flg22 treatment. Representative examples from approximately 30 roots per condition are shown.

Pathogens and Cell Death Assays. *P. syringae (Pto* DC3000 and *hrc*C) assays are described (18, 19). *Hpa* isolates Emwa1 and Noco2 were propagated as described (33) on the susceptible *Arabidopsis* ecotypes Ws and Col-0, respectively. Trypan blue staining to visualize cell death was performed as described previously (33).

ACKNOWLEDGMENTS. We thank Gregory Vert and Marc Nishimura for discussions. Anti-PR1 and anti-FLS2 antibodies were gifts from Dan Kliebenstein and Cyril Zipfel, respectively. Yves Millet in the Ausubel laboratory provided the *pCYP71A12::GUS* line. We thank Cyril Zipfel and Sacco de Vries for sharing data and ideas before publication. This work was supported by National Science Foundation Grants IOS-0649389 (to J.C.) and IOS-0929410 (to J.L.D.) and

National Institutes of Health Grant GM066025 (to J.L.D.), and by the Howard Hughes Medical Institute (J.C.). Y.B. was a Howard Hughes Medical Institute fellow of the Life Sciences Research Foundation and the recipient of the Phillipe Foundation award. Y.J. was supported by fellowships from the European Molecular Biology Organization, the F.M. Kirby Foundation, and the Stern Foundation. E.B-P. was supported by PhD and SWE fellowships from Coordenação de Aperfeiçoamento de Pessoal de Nível Superior and Conselho Nacional de Desenvolvimento Científico e Tecnológico, respectively, and by the Salk Institute. J.L.D. is a Howard Hughes Medical Institute–Gordon and Betty Moore Foundation Plant Science Investigator.

1. Jones JD, Dangl JL (2006) The plant immune system. *Nature* 444:323–329.
2. Pieterse CM, Leon-Reyes A, Van der Ent S, Van Wees SC (2009) Networking by small-molecule hormones in plant immunity. *Nat Chem Biol* 5:308–316.
3. Ronald PC, Beutler B (2010) Plant and animal sensors of conserved microbial signatures. *Science* 330:1061–1064.
4. Spoel SH, Dong X (2008) Making sense of hormone crosstalk during plant immune responses. *Cell Host Microbe* 3:348–351.
5. Vert G (2008) Plant signaling: Brassinosteroids, immunity and effectors are BAK. *Curr Biol* 18:R963–R965.
6. Wang X, et al. (2008) Sequential transphosphorylation of the BRI1/BAK1 receptor kinase complex impacts early events in brassinosteroid signaling. *Dev Cell* 15:220–235.
7. Schulze B, et al. (2010) Rapid heteromerization and phosphorylation of ligand-activated plant transmembrane receptors and their associated kinase BAK1. *J Biol Chem* 285:9444–9451.
8. Schwessinger B, et al. (2011) Phosphorylation-dependent differential regulation of plant growth, cell death, and innate immunity by the regulatory receptor-like kinase BAK1. *PLoS Genet* 7:e1002046.
9. Jaillais Y, Belkhadir Y, Balsemão-Pires E, Dangl JL, Chory J (2011) Extracellular leucine-rich repeats as a platform for receptor/coreceptor complex formation. *Proc Natl Acad Sci USA* 108:8503–8507.
10. Chinchilla D, Shan L, He P, de Vries S, Kemmerling B (2009) One for all: The receptor-associated kinase BAK1. *Trends Plant Sci* 14:535–541.
11. Nakashita H, et al. (2003) Brassinosteroid functions in a broad range of disease resistance in tobacco and rice. *Plant J* 33:887–898.
12. Nemhauser JL, Mockler TC, Chory J (2004) Interdependency of brassinosteroid and auxin signaling in Arabidopsis. *PLoS Biol* 2:E258.
13. Belkhadir Y, Chory J (2006) Brassinosteroid signaling: A paradigm for steroid hormone signaling from the cell surface. *Science* 314:1410–1411.
14. Sekimata K, et al. (2008) Brz220 interacts with DWF4, a cytochrome P450 monooxygenase in brassinosteroid biosynthesis, and exerts biological activity. *Biosci Biotechnol Biochem* 72:7–12.
15. Millet YA, et al. (2010) Innate immune responses activated in Arabidopsis roots by microbe-associated molecular patterns. *Plant Cell* 22:973–990.
16. Jaillais Y, et al. (2011) Tyrosine phosphorylation controls brassinosteroid receptor activation by triggering membrane release of its kinase inhibitor. *Genes Dev* 25: 232–237.
17. Lorrain S, Vailleau F, Balagué C, Roby D (2003) Lesion mimic mutants: Keys for deciphering cell death and defense pathways in plants? *Trends Plant Sci* 8:263–271.
18. Kim MG, et al. (2005) Two Pseudomonas syringae type III effectors inhibit RIN4-regulated basal defense in Arabidopsis. *Cell* 121:749–759.
19. Zipfel C, et al. (2004) Bacterial disease resistance in Arabidopsis through flagellin perception. *Nature* 428:764–767.
20. Zipfel C (2009) Early molecular events in PAMP-triggered immunity. *Curr Opin Plant Biol* 12:414–420.
21. Geldner N, Robatzek S (2008) Plant receptors go endosomal: A moving view on signal transduction. *Plant Physiol* 147:1565–1574.
22. Albrecht C, Russinova E, Kemmerling B, Kwaaitaal M, de Vries SC (2008) Arabidopsis somatic embryogenesis receptor kinase proteins serve brassinosteroid-dependent and -independent signaling pathways. *Plant Physiol* 148:611–619.
23. Kemmerling B, et al. (2007) The BRI1-associated kinase 1, BAK1, has a brassinolide-independent role in plant cell-death control. *Curr Biol* 17:1116–1122.
24. Knoth C, Ringler J, Dangl JL, Eulgem T (2007) Arabidopsis WRKY70 is required for full RPP4-mediated disease resistance and basal defense against Hyaloperonospora parasitica. *Mol Plant Microbe Interact* 20:120–128.
25. Sato M, et al. (2010) Network modeling reveals prevalent negative regulatory relationships between signaling sectors in Arabidopsis immune signaling. *PLoS Pathog* 6: e1001011.
26. Jaillais Y, Chory J (2010) Unraveling the paradoxes of plant hormone signaling integration. *Nat Struct Mol Biol* 17:642–645.
27. He JX, et al. (2005) BZR1 is a transcriptional repressor with dual roles in brassinosteroid homeostasis and growth responses. *Science* 307:1634–1638.
28. Michael TP, et al. (2008) A morning-specific phytohormone gene expression program underlying rhythmic plant growth. *PLoS Biol* 6:e225.
29. Wang W, et al. (2011) Timing of plant immune responses by a central circadian regulator. *Nature* 470:110–114.
30. Albrecht C, et al. (2011) Brassinosteroids inhibit PAMP-triggered immunity signaling independent of the *Arabidopsis* LRR-RLK BAK1. *Proc Natl Acad Sci USA*, in press.
31. Symons GM, Reid JB (2004) Brassinosteroids do not undergo long-distance transport in pea. Implications for the regulation of endogenous brassinosteroid levels. *Plant Physiol* 135:2196–2206.
32. Kemen E, et al. (2011) Gene gain and loss during evolution of obligate parasitism in the white rust pathogen of Arabidopsis thaliana. *PLoS Biol* 9:e1001094.
33. Holt BF, III, Belkhadir Y, Dangl JL (2005) Antagonistic control of disease resistance protein stability in the plant immune system. *Science* 309:929–932.

Supporting Information

Belkhadir et al. 10.1073/pnas.1112840108

SI Experimental Procedures

Plant Cultivation, Ecotypes, and Mutants. The WT used in all experiments was *A. thaliana* accession Col-0. The *A. thaliana* accession Wassilewskija (Ws-0) was used as a control in Fig. 5. Plants were grown on soil or Petri dishes containing 0.5× Linsmaier and Skoog medium (Caisson Laboratories) in long-daylight conditions. For pathogen assays, plants were grown in growth chambers in short-day conditions. The following mutant plant genotypes were used in this work: *bak1-3* (1), *bri1* (GABI_134E10) (2), *fls2* (SALK_026801c), and *rpp4* (3). The insertion sites for the T-DNA lines (SALK_026801c) was located in the ORF of *FLS2*. Homozygosity of the *fls2* mutation and the sequence of the insertion site were confirmed by PCR and sequencing. The *fls2* mutant was confirmed to be a null allele by Western blot by using native anti-FLS2 polyclonal antibodies. The *sud1* allele has been described previously (4).

Transgenic Lines, Constructs, and Phenotypic Analysis. *BRI1*, *BAK1*, and *BKI1* tagged variant (mCitrine, mCherry, and HA tags) constructs were generated as described previously (2). Site-directed mutagenesis to generate the $BRI1^{sud1}$*mCitrine* allele was carried out following the site-directed mutagenesis protocol from Agilent Technology (formerly Stratagene), and the primers used are: sud1 forward (G643E), ACTAGCAGAGTCTATGAAGGTCACACTT C GCCG; and sud1 reverse (G643E), TGATCGTCTCAGATA CTTCCAGTGTGAAGCGGC. The constructs created and used are listed in Table S3. *BRI1* and *BAK1* constructs were transformed into WT Col-0, heterozygous *bri1* (2), and homozygous *bak1-3,* respectively, and their transgenic expression fully rescued the *bri1* and *bak1* dwarfism. For all constructs, more than 20 independent T1 lines were isolated and three to eight representative single insertion lines were selected in the T2 generation. Confocal microscopy, phenotypic analysis, and protein extraction were performed on segregating T2 and homozygous T3 lines as described previously (2). The functional *FLS2prom::FLS2::GFP* in Col-0 is a gift from Silke Robatzek (The Sainsbury Laboratory, Norwich, UK) (5). The *35S::DWF4* line in Col-0 was described previously (6). Table S2 includes a list and sources of transgenic lines used in this study.

Protein Analysis. Polyclonal anti-FLS2 antibodies were used at dilutions of 1:2,000 for immunodetection assays and 1:500 for immunoprecipitation (IP) assays. Antiphosphothreonine antibodies were used according to the manufacturer's instruction (Novagen). Protein extraction and quantification was performed as described previously (7); approximately 100 mg of 14-d-old light-grown seedlings were harvested for Western blot experiments. IP experiments were performed as described previously (8). Briefly, IP experiments required 1 g of seedlings (14 d old). Flash-frozen tissues were ground at 4 °C in a 15-mL tube containing 2 mL of ice-cold sucrose buffer [20 mM Tris, pH 8; 0.33 M sucrose; 1 mM EDTA, pH 8; protease inhibitor (Roche)] using a Polytron homogenizer (Brinkmann). Samples were centrifuged for 10 min at 5,000 × *g* at 4 °C or until the supernatants were clear. These total protein fractions were centrifuged at 4 °C for 45 min at 20,000 × *g* to pellet microsomes. The pellet was resuspended in 1 mL of IP buffer (20 mM Tris, pH 8, 0.33 M Sucrose, 150 mM NaCl, 0.5% Triton X-100) by using a 2-mL Potter–Elvehjem homogenizer.

Quantitative RT-PCR Analyses. Total RNA was isolated from frozen tissue (liquid nitrogen) by using the Spectrum Plant Total RNA Kit (cat. no. STRN250-1KT; Sigma) according to the manufacturer's instructions. One microgram of total RNA was added to each cDNA synthesis reaction using the First-Strand cDNA Synthesis Kit (cat. no. K1611; Fermentas). For quantitative real-time PCR, cDNA was synthesized, and DNA amplification was performed in the presence of SYBR Green qPCR Detection (Invitrogen) on the MyIQ Single Color Real-Time PCR Detection System (BioRad), using the following primer pairs: *WRK11* forward, ATGTCCAGCGAGGAAACACGT; reverse, TATTCTCCTGCATCGCGGATT; *WRKY6* forward, 5′-CAT ATTACCGCTGCACGATGG-3′; reverse, 5′-GGCAACGGATGGTTATGGTTT-3′; *WRKY29* forward, 5′-TTCGTTTTGCCTACCGATGG-3′; reverse, 5′-CGAGCTTGTGAGGATCGTTTG-3′; *WRK53* forward, 5′-AAATCCCGGCAGTGTTCCA-3′; reverse, 5′-TCTTGGCGATGATGACTCTCG-3′; *ACTIN 2/8* forward, 5′-TCTTGTTCCAGCCCTCGTTT-3′; reverse, 5′-TCTCGTGGATTCCAGCAGCT-3′; and *18S rRNA* forward, 5′-TATAGGACTCCGCTGGCACC-3′; reverse, 5′-CCCGGAACCCAAAAACTTTG-3′. The cycle used was: 95 °C for 1 min 30 s; 40× (95 °C for 10 s; 60 °C for 1 min); 95 °C for 1 min; 60 °C for 1 min and 81× (60 °C for 10 s). The relative mRNA levels were determined by normalizing the PCR threshold cycle number with actin and 18S rRNA. All experiments were repeated three times independently, and the average was calculated.

Pathogens and Cell Death Assays. *Pto* DC3000 and *hrc*C have been described previously (5). Bacterial growth in plant leaves was assessed by inoculating 4-wk-old plants with 10^5 cfu/mL. Growth inhibition of *Pto* DC3000 and *hrc*C by flg22 was conducted as described previously (8). Briefly, bacteria at a concentration of 10^5 cfu/mL were coinoculated with 1 μM flg22. For each sample, four leaf discs were pooled three times per data point (12 leaf discs total). Leaf discs were cored from the infiltrated area and ground to homogeneity in 10 mM $MgCl_2$, and the bacterial titer determined by serial dilution and plating. This experiment was repeated three times with consistent results. For *Hpa* sporangiophore growth assays, 12-d-old seedlings were inoculated with 32,000 spores/mL of the virulent *Hpa* isolate Noco2 or the avirulent isolate Emwa1. Plants were kept covered with a lid to increase humidity and grown at 20 °C with a 9-h light period. Sporangiophores were counted at 4 dpi (*Hpa* Noco2) or 5 dpi (*Hpa* Emwa1) by using a dissecting microscope (M205 FA; Leica). To evaluate infection in cotyledons, sporangiophores were counted on the adaxial and abaxial surfaces (9). Sporangiophores on primary leaves were counted only on the adaxial surface, as infected leaves often showed a strong epinastic phenotype. Trypan blue staining was performed to visualize cell death as described previously (4).

1. Jaillais Y, Belkhadir Y, Balsemão-Pires E, Dangl JL, Chory J (2011) Extracellular leucine-rich repeats as a platform for receptor/coreceptor complex formation. *Proc Natl Acad Sci USA* 108:8503–8507.
2. Jaillais Y, et al. (2011) Tyrosine phosphorylation controls brassinosteroid receptor activation by triggering membrane release of its kinase inhibitor. *Genes Dev* 25:232–237.
3. Knoth C, Ringler J, Dangl JL, Eulgem T (2007) Arabidopsis WRKY70 is required for full RPP4-mediated disease resistance and basal defense against Hyaloperonospora parasitica. *Mol Plant Microbe Interact* 20:120–128.
4. Hothorn M, et al. (2011) Structural basis of steroid hormone perception by the receptor kinase BRI1. *Nature* 474:467–471.
5. Robatzek S, Chinchilla D, Boller T (2006) Ligand-induced endocytosis of the pattern recognition receptor FLS2 in Arabidopsis. *Genes Dev* 20:537–542.
6. Lorrain S, Vailleau F, Balagué C, Roby D (2003) Lesion mimic mutants: Keys for deciphering cell death and defense pathways in plants? *Trends Plant Sci* 8:263–271.
7. Belkhadir Y, et al. (2010) Intragenic suppression of a trafficking-defective brassinosteroid receptor mutant in Arabidopsis. *Genetics* 185:1283–1296.
8. Belkhadir Y, Nimchuk Z, Hubert DA, Mackey D, Dangl JL (2004) Arabidopsis RIN4 negatively regulates disease resistance mediated by RPS2 and RPM1 downstream or independent of the NDR1 signal modulator and is not required for the virulence functions of bacterial type III effectors AvrRpt2 or AvrRpm1. *Plant Cell* 16:2822–2835.

9. Zipfel C, et al. (2004) Bacterial disease resistance in Arabidopsis through flagellin perception. *Nature* 428:764–767.

10. Symons GM, Reid JB (2004) Brassinosteroids do not undergo long-distance transport in pea. Implications for the regulation of endogenous brassinosteroid levels. *Plant Physiol* 135:2196–2206.

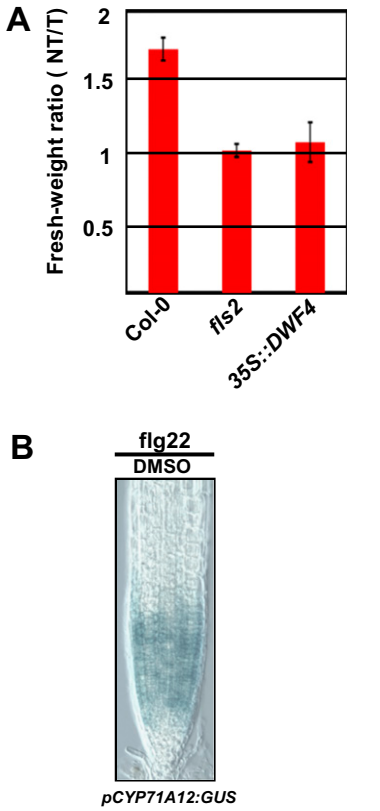

Fig. S1. Interplay between BR- and flg22-induced signaling. (*A*) Increased BR concentrations prevent flg22-induced growth inhibition. The red bar represents the average fresh-weight ratio of 14-d-old seedlings of the indicated genotypes grown for 7 d in water (NT) or 1 μM flg22 (T). Means and SDs were calculated from approximately 48 seedlings (six random pools of eight seedlings). This experiment was repeated three times with similar results. (*B*) Control GUS stain of the *CYP71A12::GUS* line. Seedlings were grown in the presence of DMSO the BRZ solvent and treated with 1 μM flg22 for 12 h before GUS staining.

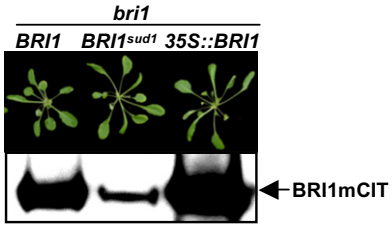

Fig. S2. Gain-of-function mutations in *BRI1* promote BR-independent cell elongation. Representative pictures of rosette stage transgenic *bri1* plants (T3) expressing *BRI1* or *BRI1*^{sud1} under the control of the native promoter or the CaMV35S promoter (*35S::BRI1*). The phenotypes associated with the overexpression of *BRI1* (*35S::BRI*)—narrow leaf blades and elongated and twisting petioles—were recapitulated by driving the expression of the BRI1^{sud1} variant under the control of the native promoter. *Bottom*: Microsomal protein extracts were prepared from *BRI1mCIT bri1*, *BRI1*^{sud1}*mCIT bri1*, and *35S::BRI1mCIT bri1* plants. These extracts were subjected to an anti-GFP protein immunoblot analysis to detect the accumulation of the mCitrine-tagged proteins. Equal loading was ensured by protein quantification before loading.

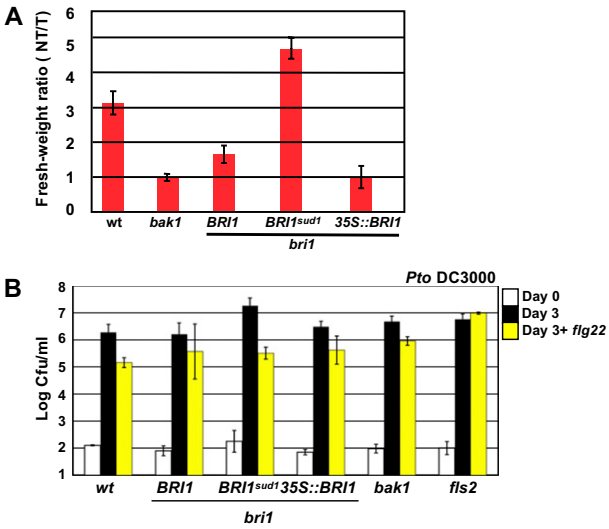

Fig. S3. BR signaling modulates responses to MAMPs. (*A*) The red bar represents the average fresh-weight ratio of 14-d-old seedlings of the genotypes indicated at the bottom grown for 7 d in water (NT) or 1 μM flg22 (T). Means and SDs were calculated from approximately 48 seedlings (six random pools of eight seedlings). This experiment was repeated three times with similar results. (*B*) Growth of *Pto*DC3000 was measured in the genetic backgrounds indicated at the bottom of the chart. Four-week-old plants were infiltrated with 10^5 cfu/mL *Pto*DC3000 in the presence (yellow bars) or absence (black bars) of 1 μM flg22. The number of bacteria per area of leaf was determined at 0 and 3 dpi. Values are mean cfu/mL; error bars represent ± 2 SE calculated from four internal replicate samples.

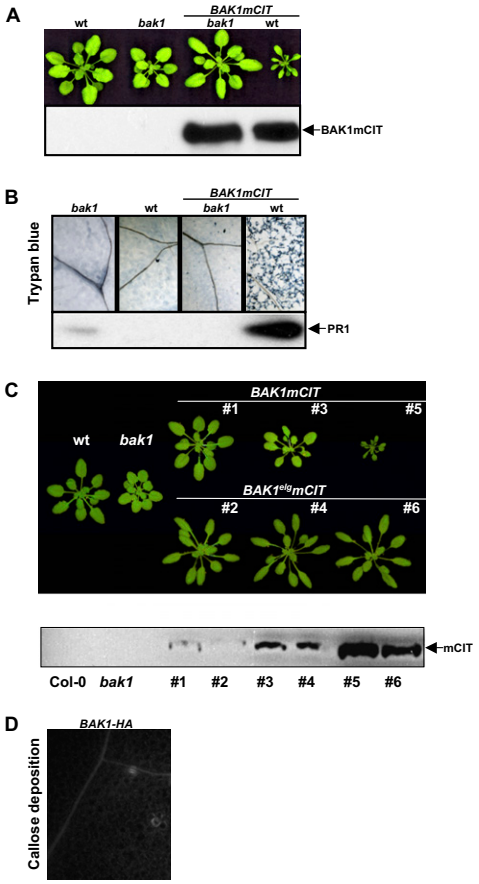

Fig. S4. Overexpression of *BAK1,* but not *BAK1^{elg}*, triggers inappropriate plant cell death. (*A*) *Top*: Images of representative rosettes of the genotypes listed. Functional complementation was confirmed by phenotypic rescue of the moderate dwarf phenotype of *bak1* in transgenic plants expressing *BAK1mCitrine* from the native promoter. *Bottom*: Microsomal protein extracts were prepared from the genotypes listed at the top. These extracts were subjected to anti-GFP immunoblot analysis to detect mCitrine-tagged proteins. Bradford protein quantification assay were used to confirm equal loading. (*B*) *Top*: Representative examples of 30 to 40 leaves of independent plants from each genotype listed at the top were trypan blue-stained and microscopically analyzed for cell death occurrence. *Bottom*: Total protein extracts were prepared from the genotypes listed at the top and subjected to anti-PR1 immunoblot. (*C*) *Top*: Images of representative rosettes of the genotypes listed in white expressing various levels of mCitrine-tagged *BAK1* (BAK1mCIT) and *BAK1^{elg}* (BAK1^{elg}mCIT) under the control of its native promoter. *Bottom*: Microsomal protein extracts were prepared from the genotypes listed in white and subjected to anti-GFP immunoblot analysis to detect mCitrine-tagged proteins. Plants expressing equivalent levels of BAK1 and BAK1^{elg} are matched from top to bottom (nos. 1 and 2, nos. 3 and 4, nos. 5 and 6). (*D*) Control aniline blue-stained callose deposits in the leaves of BAK1-HA plants treated with 1/2MS, but not flg22. This line was used for the cross with BRI1mCIT plants (Fig. 3*B*). Importantly, this *BAK1-HA* plant line does not display constitutive callose deposition.

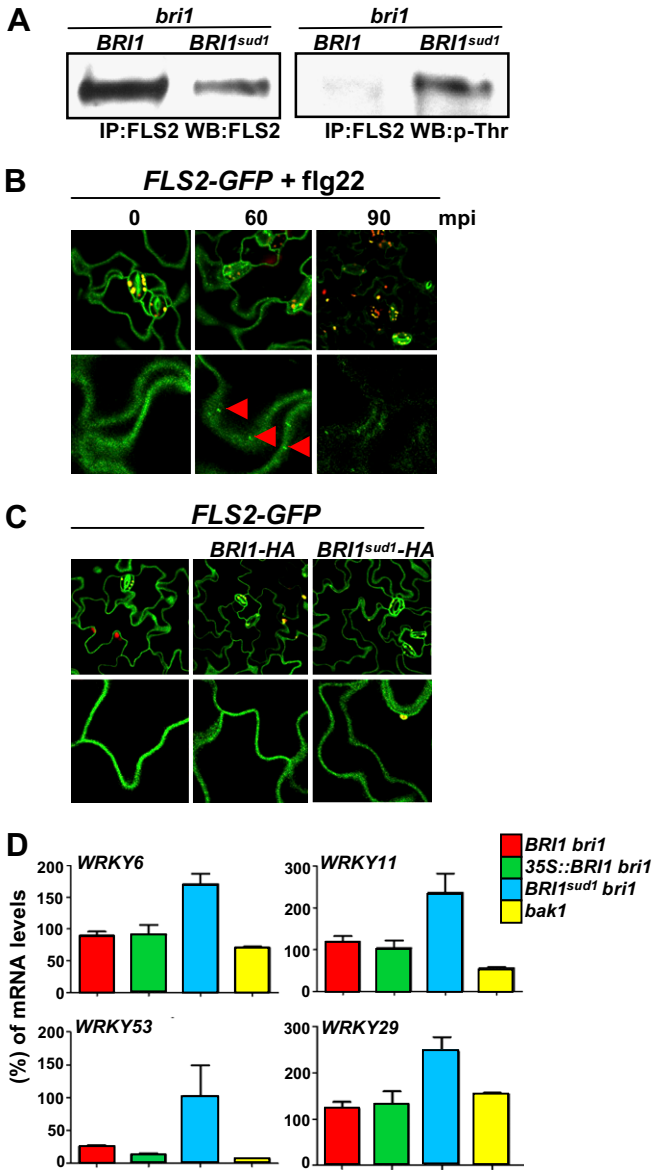

Fig. S5. *BRI1*^{sud1} affects FLS2 activation state and basal defenses gene expression. (*A*) Microsomal protein extracts prepared from *BRI1* and *BRI1*^{sud1}*mCIT* seedlings were immunoprecipitated with anti-FLS2 antibody (IP; FLS2) and analyzed with anti-FLS2 antibody (WB; FLS2) or antiphosphothreonine antibody (WB; p-Thr). (*B*) Intracellular dynamics of FLS2-GFP in response to flg22. Two-week-old FLS2-GFP seedlings were treated with a solution of 10 μM flg22. GFP signal was monitored over a period of 90 min by confocal microscopy of leaf epidermal cells. Red arrows show the appearance of nascent endosomes. Our results confirm previously published results demonstrating that FLS2 is internalized and disappears upon flg22 treatment (5). (*C*) *FLS2-GFP BRI1-HA* or *FLS2-GFP BRI1*^{sud1}*-HA* double transgenic lines were constructed by crossing an FLS2-GFP line to homozygous T2 plants transformed with an HA epitope-tagged *BRI1* transgene driven by the native promoter. FLS2 localization and internalization state was monitored in the absence of flg22. Our results indicate that the steady-state distribution of FLS2 intracellular pools is not modified in *BRI1*^{sud1} plants. (*D*) Quantitative real-time PCR analyses of the indicated *WRYK* transcripts from seedlings of the genotypes listed on the right.

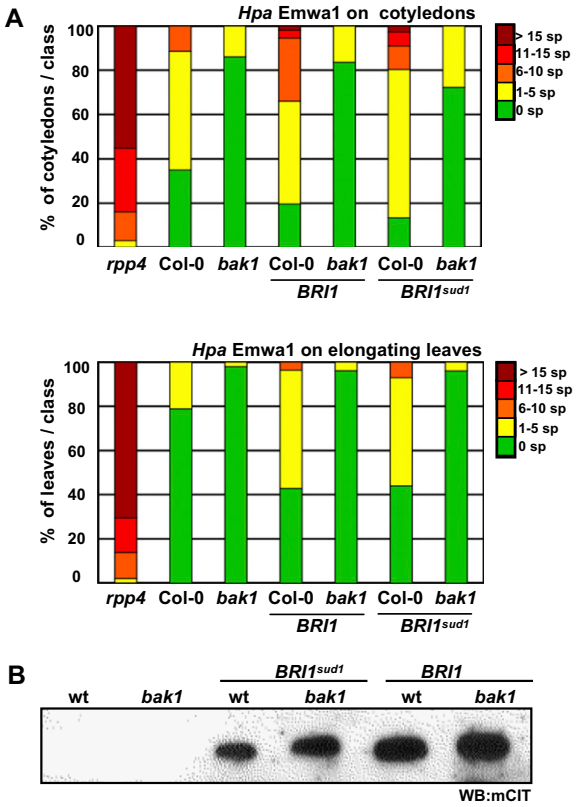

Fig. S6. Enhanced BR signaling affects RPP4-mediated resistance in a BAK1-dependent manner. (*A*) Twelve-day-old cotyledons of the genetic backgrounds indicated at the bottom of the chart were inoculated with conidiospores of the avirulent *Hpa* isolate Emwa1 at 32,000 spores/mL. Sporangiophores were counted 5 d after inoculation on cotyledons (*Upper*) and first true leaves (*Lower*) for each of the indicated genetic backgrounds. Means, sample size, and 2 × SE are presented in Table S1. Note that the T2 *BRI1mCitrine* (*BRI1*) or *BRI1*^{sud1}*mCitrine* (*BRI1*^{sud1}) plants express *BRI1* under the control of the native promoter in the WT (Col-0) or *bak1* genetic backgrounds. sp, sporangiophores per cotyledon (*Top*) or sporangiophores per leaf (*Bottom*). (*B*) Microsomal protein extracts were prepared from the genotypes listed at the top. These extracts were subjected to an anti-GFP protein immunoblot analysis to detect the accumulation of the mCitrine-tagged proteins (*Bottom*). Equal loading was ensured by protein quantification before loading.

Table S1. Raw data from *Hpa* assays

	Hpa Noco2 32,000 spores/mL 4 dpi						*Hpa* Emwa1 32,000 spores/mL 5 dpi					
	Cotyledons			Primary leaves			Cotyledons			Primary leaves		
	With sporangiophores, %	Mean ± 2 SE	Sample size*	With sporangiophores, %	Mean ± 2 SE	Sample size*	With sporangiophores, %	Mean ± 2 SE	Sample size*	With sporangiophores, %	Mean ± 2 SE	Sample size*
Ws	0.0	0.0 ± 0.0	81	0.0	0.0 ± 0.0	40	ND	ND	ND	ND	ND	ND
rpp4	ND	ND	ND	ND	ND	ND	100.0	15.9 ± 0.5	100	100.0	17.3 ± 0.7	51
Col-0	80.2	8.2 ± 0.7	101	88.9	9.3 ± 0.9	72	64.9	2.2 ± 0.2	114	21.1	0.2 ± 0.1	57
bak1	60.9	5.0 ± 0.7	92	65.0	4.6 ± 0.7	60	13.9	0.2 ± 0.1	115	2.0	0.0 ± 0.0	51
BRI1	86.7	11.5 ± 0.8	105	98.1	16.6 ± 0.8	52	80.4	4.2 ± 0.4	112	57.1	1.3 ± 0.2	56
BRI1 bak1	40.2	1.5 ± 0.3	97	38.5	2.9 ± 0.7	52	16.3	0.2 ± 0.0	104	5.8	0.0 ± 0.0	53
BRI1 ^{sud1}	88.2	11.1 ± 0.8	102	92.6	14.6 ± 1.0	54	86.6	3.8 ± 0.4	112	56.1	1.4 ± 0.3	57
BRI1 ^{sud1} *bak1*	42.1	2.5 ± 0.5	95	49.0	3.0 ± 0.6	51	27.7	0.4 ± 0.1	101	5.9	0.0 ± 0.0	51

ND, not detected.

*No. of cotyledons or primary leaves.

Table S2. Transgenic lines tested in this study

Transgenic line	Promoter	Epitope tag/gene fusion	Genetic background	Ref.
35S::DWF4	35S CaMV	None	Col-0	1
pCYP71A12::GUS	*CYP71A12* native promoter	GUS	Col-0	2
BRI1	BRI1 native promoter	mCitrine	Col-0	3
BRI1 bri1	BRI1 native promoter	mCitrine	*bri1* T-DNA null	3
BRI1 bak1	BRI1 native promoter	mCitrine	bak1-3 null	Present study
BRI1sud1	BRI1 native promoter	mCitrine	Col-0	Present study
BRI1sud1 bri1	BRI1 native promoter	mCitrine	*bri1*T-DNA null	Present study
BRI1sud1 bak1	BRI1 native promoter	mCitrine	bak1-3	Present study
BRI1-HA	BRI1 native promoter	HA	Col-0	3
BRI1sud1-HA	BRI1 native promoter	HA	Col-1	Present study
35S::BRI1 bri1	35S CaMV	mCitrine	*bri1* T-DNA null	Present study
BAK1-HA	BAK1 native promoter	HA	Col-0	Present study
BAK1mCIT	BAK1 native promoter	mCitrine	Col-0	3, 4
BAK1mCIT bak1	BAK1 native promoter	mCitrine	bak1-3 null	4
BAK1mCHE	BAK1 native promoter	mCherry	Col-0	3
BKI1mCIT	UBIQUITIN promoter	mCitrine	Col-0	3
FLS2-GFP	FLS2 native promoter	GFP	Col-0	5

1. Nemhauser JL, Mockler TC, Chory J (2004) Interdependency of brassinosteroid and auxin signaling in Arabidopsis. *PLoS Biol* 2:E258.
2. Millet YA, et al. (2010) Innate immune responses activated in Arabidopsis roots by microbe-associated molecular patterns. *Plant Cell* 22:973–990.
3. Jaillais Y, et al. (2011) Tyrosine phosphorylation controls brassinosteroid receptor activation by triggering membrane release of its kinase inhibitor. *Genes Dev* 25:232–237.
4. Jaillais Y, Belkhadir Y, Balsemão-Pires E, Dangl JL, Chory J (2011) Extracellular leucine-rich repeats as a platform for receptor/coreceptor complex formation. *Proc Natl Acad Sci USA* 108: 8503–8507.
5. Robatzek S, Chinchilla D, Boller T (2006) Ligand-induced endocytosis of the pattern recognition receptor FLS2 in Arabidopsis. *Genes Dev* 20:537–542.

Table S3. Plasmid constructs used in this study

Construct name	Binary vector	Resistance in plant
BAK1prom::BAK1-mCITRINE (BAK1-CITRINE)	*pB7m34GW*	Basta
BAK1prom::BAK1-mCHERRY (BAK1-CHERRY)	*pH7m34GW*	Hygromycin
BAK1prom::BAK1-6xHA (BAK1-6xHA)	*pK7m34GW*	Kanamycin
35Sprom::BRI1-CITRINE (OxBRI1-CITRINE)	*pB7m34GW*	Basta
BRI1prom::BRI1-mCITRINE (BRI1-mCITIRINE)	*pB7m34GW*	Basta
BRI1prom::BRI1-6xHA (BRI1-6xHA)	*pK7m34GW*	Kanamycin
BRI1prom::BRI1sud1-mCITRINE (BRI1sud1-mCITRINE)	*pB7m34GW*	Basta
BRI1prom::BRI1sud1-6xHA (BRI1sud1-6xHA)	*pK7m34GW*	Kanamycin
UBQ10prom::BKI1-mCITRINE (BKI1-mCITRINE)	*pB7m34GW*	Basta

Further details are provided in Jaillais et al. (1).

1. Jaillais Y, et al. (2011) Tyrosine phosphorylation controls brassinosteroid receptor activation by triggering membrane release of its kinase inhibitor. *Genes Dev* 25:232–237.